SAND2019-13758J

AUTHOR QUERY FORM

AIP Publishing	Journal: Appl. Phys. Lett. Article Number: APL19-AR-06367	Please provide your responses and any corrections by annotating this PDF and uploading it to AIP's eProof website as detailed in the Welcome email.

Dear Author,

Below are the queries associated with your article; please answer all of these queries before sending the proof back to AIP.

Article checklist: In order to ensure greater accuracy, please check the following and make all necessary corrections before returning your proof.

1. Is the title of your article accurate and spelled correctly?
2. Please check affiliations including spelling, completeness, and correct linking to authors.
3. Did you remember to include acknowledgment of funding, if required, and is it accurate?

Location in article	Query / Remark: click on the Q link to navigate to the appropriate spot in the proof. There, insert your comments as a PDF annotation.
AQ1	Please check that the author names are in the proper order and spelled correctly. Also, please ensure that each author's given and surnames have been correctly identified (given names are highlighted in red and surnames appear in blue).
AQ2	Please provide complete details for Ref. 10.
AQ3	Please provide volume number for Ref. 14.
AQ4	We were unable to locate a digital object identifier (doi) for Ref(s). 2, 19, 25, 26, 28, 32 and 39. Please verify and correct author names and journal details (journal title, volume number, page number, and year) as needed and provide the doi. If a doi is not available, no other information is needed from you. For additional information on doi's, please select this link: http://www.doi.org/.
	If you wish to add an ORCID for any author that does not have one, you may do so now. For more information on ORCID, see https://orcid.org/. John A. Tomko- David R. Boris- Samantha G. Rosenberg- Scott G. Walton- Patrick E. Hopkins-
	Please check and confirm the Funder(s) and Grant Reference Number(s) provided with your submission: Office of Naval Research Global, Award/Contract Number N00014-15-1-2769 U.S. Naval Research Laboratory, Award/Contract Number Base program Please add any additional funding sources not stated above:

Thank you for your assistance.

Sandia National Laboratories is a multimission laboratory managed and operated by National Technology & Engineering Solutions of Sandia, LLC, a wholly owned subsidiary of Honeywell International Inc., for the U.S. Department of Energy's National Nuclear Security Administration under contract DE-NA0003525.

J_ID: APPLAB DOI: 10.1063/1.5120028 Date: 22-October-19 Stage: Page: 1 Total Pages: 6

PROOF COPY [APL19-AR-06367]

Applied Physics Letters ARTICLE scitation.org/journal/apl

Thermal conductance of aluminum oxy-fluoride passivation layers

Cite as: Appl. Phys. Lett. **115**, 000000 (2019); doi: 10.1063/1.5120028
Submitted: 16 July 2019 · Accepted: 18 October 2019 ·
Published Online: 0 Month 0000

AQ1 John A. Tomko,[1] David R. Boris,[2] Samantha G. Rosenberg,[3] Scott G. Walton,[2] and Patrick E. Hopkins[1,4,5,a)]

AFFILIATIONS

[1]Department of Materials Science and Engineering, University of Virginia, Charlottesville, Virginia 22903, USA
[2]Plasma Physics Division, Naval Research Laboratory, 4555 Overlook Ave. SW, Washington DC 20375, USA
[3]ASEE Postdoctoral Research Associate, U.S. Naval Research Laboratory, 4555 Overlook Ave. SW, Washington, DC 20375, USA
[4]Department of Mechanical Engineering, University of Virginia, Charlottesville, Virginia 22903, USA
[5]Department of Physics, University of Virginia, Charlottesville, Virginia 22903, USA

[a)]Author to whom correspondence should be addressed: phopkins@virginia.edu

ABSTRACT

The thermal properties of plasma-generated aluminum oxy-fluoride passivation layers at the surface of aluminum thin films are measured. The oxy-fluoride layers are generated using plasmas produced in mixtures of NH_3 and SF_6 to simultaneously remove oxygen and add fluorine to the aluminum surface, an alternative approach to the more conventional two-step methods that utilize HF treatments to remove the native oxide followed by metal-fluoride (e.g., MgF_2, LiF, and AlF_3) thin film deposition that serves to protect the aluminum surface from further oxidation. Here, the change in thermal properties of the layers as a function of plasma processing time is determined. A significant reduction in thermal boundary conductance is measured with the increasing treatment time, which can be related to the increasing fluorine content in the layers. Acoustic reflection measurements indicate this reduced thermal boundary conductance is associated with lower bonding strength to aluminum with increasing fluorine.

The predominant failure mechanisms in thin film optical devices and materials arise from thermomechanical effects within the lens, mirror, etc.[1,2] For example, a typical mirror is composed of a thin aluminum film on a given substrate; upon reflection of light, a portion of the photon energy is absorbed by the metal film, which creates a temperature rise on the surface.[3] To avoid the aforementioned thermomechanical failure, it is common to utilize a high thermal conductivity substrate to dissipate heat from the film surface into the bulk of the substrate[4] and thus avoid damaging effects due to energy confinement, thermal buildup, and increased temperatures. While this works in certain regimes, a large number of works have shown that the damage threshold from high-power laser interactions,[5] flip-chip photodiodes,[6] and other electronic devices does not necessarily scale with the thermal conductivity of the underlying substrate. Rather, the thermal resistance of the interface[7,8] between the thin film and its supporting substrate becomes a limiting factor and defines the threshold at which these devices or material systems undergo thermal failure.

Aluminum is a good choice of material for UV optics due to its excellent reflectivity to wavelengths as short as 90 nm. Unfortunately, the native oxide layer that readily forms on aluminum severely degrades the performance of aluminum reflectors. A promising solution is the use of fluorine-containing layers that protect the aluminum from oxidation and provide high transmission.[9–11] Further, aluminum fluoride layers are useful as barrier coatings in advanced Li-ion battery architectures, where localization of large temperature rise and thermal runaway are predominant failure mechanisms.[12] To date, the thermal properties of aluminum fluoride thin films have yet to be reported, leaving the potential for unknown thermal degradation of these materials.

In this work, we measure the thermal properties of thin aluminum oxyfluoride (AlO_xF_y) layers on the surface of aluminum films evaporated on glass substrates using time-domain thermoreflectance (TDTR); this optical pump-probe technique measures both the thermal resistance of the AlO_xF_y layer and the thermal boundary conductance (TBC) associated with the interface comprising AlO_xF_y and its underlying aluminum substrate.[13,14] Furthermore, this method allows for the measurement of acoustic reflection from AlO_xF_y, providing additional insight into the mechanical and adhesive properties of the AlOxFy film.[15–17]

AlO_xF_y layers were prepared by plasma treatment of bare Al coatings on glass substrates in the U.S. Naval Research Laboratory's

(NRL) Large Area Plasma Processing System (LAPPS).[18,19] The system makes use of linear hollow cathode electron sources to generate sheet-like electron beams with typical current densities of 1–5 mA/cm^2 and beam energies between 1 and 5 keV. Coaxial magnetic fields of 100–300 Gauss are used to collimate the electron beam and thus improve uniformity along its length.[20] These parameters are sufficient to produce uniform plasma sheets compatible with typical wafer-scale systems (diameter > 300 mm). LAPPS is able to generate uniform, very low electron temperature, T_e (<1 eV), plasmas with densities in the range of 10^{10}–10^{12} cm^{-3}, thus providing the ability to deliver a well-controlled flux of ions characterized by very low energies (<5 eV) to material surfaces located adjacent to the plasma sheet.[21] The low ion energies serve to preserve surface morphology and practically eliminate ion-induced damage during processing. For this work, LAPPS was combined with an auxiliary discharge, which serves to dissociate the working gas as it enters the reactor and provides additional control over the ratio of ions to reactive neutrals incident on the surface.[22]

Gas mixtures of argon (Ar), sulfur-hexafluoride (SF_6), and ammonia (NH_3) were used to treat aluminum thin films deposited on glass. This gas mixture was passed through an inductively couple plasma (ICP) discharge source operating at 350 W, which significantly increases the relative concentration of F radicals in the reactor[22] compared to the use of the electron beam alone.[23,24] This mixture was chosen to provide both a large flux of F atoms and HF radicals to the surface. The latter is likely formed through hydrogen abstraction from the NH_3 molecule by F atoms. Evidence for the production of gas-phase HF, known to be highly effective at removing oxygen from surfaces and fluorinating Al_2O_3,[25,26] is shown in Fig. 1.

The material systems studied in this work are fabricated from an 80 nm thick aluminum electron-beam evaporated on fused quartz (SiO_2 glass) substrates at a chamber pressure of 10^{-6} Torr; the glass substrate is alcohol cleaned followed by an O_2 plasma treatment prior to deposition. The native oxide layer develops on the surface of the Al film due to exposure to the ambience prior to plasma treatment. Pre and post-treatment X-Ray Photo-electron Spectroscopy (XPS) measurements, shown in Table I, show a plasma exposure of 240 s transforms the native oxide layer (Al_2O_3) into a Fluorine-rich (AlO_xF_y) layer at the surface. From analysis of the high-resolution spectra (not shown), we estimate the AlF_xO_y layer to be less than 5 nm in thickness. That is to say, the plasma treatment involves the conversion of the native oxide layer, Al_2O_3, into an AlF_xO_y layer of comparable thickness. As was the case for a variety of material systems in previous works,[27,28]

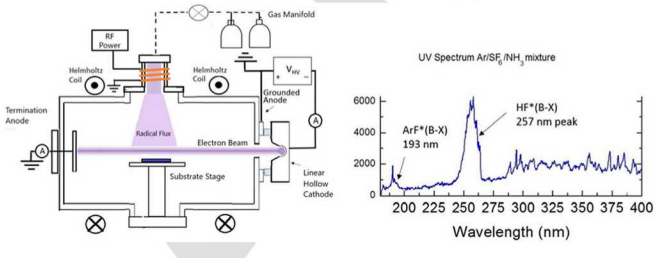

FIG. 1. (left) Schematic of the LAPPS configuration with an auxiliary inductively coupled plasma radical source. (right) UV spectrum of $Ar/SF_6/NH_3$ plasma showing the presence of excited HF molecules.

TABLE I. Surface composition via XPS for varying plasma chemistry.

Plasma chemistry	% Al (XPS)	% O (XPS)	% F (XPS)	% C (XPS)	Treatment time (s)
$Ar/SF_6/NH_3$ 150 sccm/4.4 sccm/ 1.8 sccm	22.3%	30.2%	44.2%	3.3%	240
As-received sample	35.3%	60.1%	0%	4.6%	0

the F concentration scales with dose, and so it is reasonable to expect that the F concentration increases with plasma exposure times.

To ensure proper sensitivity in our TDTR measurements to the conductance of the thin AlO_yF_x on the surface of the Al film, we electron-beam evaporate an additional 80 ± 4 nm Al film onto the AlO_yF_x layer. This additional film thus acts as our optothermal transducer during the thermal measurements and provides symmetry about the AlO_yF_x layer, as equivalent TBCs at both Al/AlO_yF_x interfaces can be assumed. To assure sample-to-sample consistency, both the initial Al film and the final Al transducer for all samples are created in a single deposition. The remaining ~5% deviation in the film thickness across the sample surface is the primary source of uncertainty in our TDTR measurements, and the values of thermal conductance are obtained through the oxyfluoride layer and its respective interfaces.

As shown in Fig. 2, we find over a twofold decrease in the measured thermal conductance after 240 s of plasma treatment; this thermal conductance is composed of the thermal resistance of the interface layer itself (Al_2O_3 or AlO_yF_x) as well as the TBC between the top and underlying Al films. In other words, assuming no change in the thermal conductivity of the passivation layer relative to the native oxide, the thermal conductance of an Al/Al_2O_3 interface is found to be approximately two times greater than the thermal conductance across an Al/AlO_yF_x interface; more on this TBC reduction is discussed below.

More rigorously for this experimental geometry, the measured thermal conductance, G, can be represented as a series thermal resistance, given by

$$G_{measured} = \left(\frac{2}{TBC} + \frac{d}{\kappa}\right)^{-1}, \quad (1)$$

where TBC is simply the thermal boundary conductance between the Al films and the AlO_yF_x layer, while κ and d are the thermal conductivity and thickness of the AlO_yF_x layer, respectively. Note the factor of two arises from the assumption of interfacial symmetry about the intermediate layer.

We begin by considering the case of the native oxide, Al_2O_3, at zero processing times. There are two limiting cases regarding the thermal conductivity in this equation: pure, crystalline Al_2O_3 with a thermal conductivity of ≈35 W m^{-1} K^{-1} and fully amorphous, dense Al_2O_3 at not less than ≈1 W m^{-1} K^{-1}.[29] With these limits, we find that the measured TBC at the Al/Al_2O_3 interface is 220–330 W m^{-1} K^{-1}. These values are within the limits of previously measured Al/Al_2O_3 TBCs and are on par with diffuse mismatch model calculations in previous works.[8]

In the case of Al/AlO_yF_x interfaces, there are no previous values from 'bulk' thermal conductivity measurements. Furthermore, the

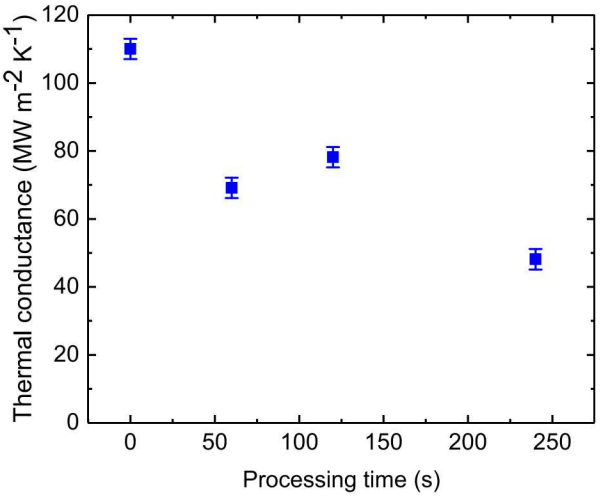

FIG. 2. Measured thermal conductance as a function of plasma processing time for conversion of native Al_2O_3 (zero process time) into AlO_yF_x coatings. This represents the effective conductance of the two Al/AlO_yF_x interfaces as well as the intrinsic thermal resistance of the AlO_yF_x layer. Regardless, over a factor of two change is found relative to the native Al_2O_3 film (i.e., zero processing time).

assumption of a crystallinelike thermal conductivity for these plasma-processed layers is most likely not applicable; numerous works have shown that AlF_3 and AlO_yF_x layers and coatings are amorphous and lack long-range symmetry.[30–33] While the degree of crystallinity of these oxyfluoride layers is unknown, we can determine realistic bounds for the thermal boundary conductance of the Al/AlO_yF_x interface. Based on the minimum limit to the thermal conductivity of amorphous solids,[34] a fully amorphous AlO_yF_x layer has a thermal conductivity of likely not less than 1 W m^{-1} K^{-1}, whereas a fully crystalline structure would not exceed that of its crystalline oxide counterpart (35 W m^{-1} K^{-1}). Repeating the same series thermal resistor approach for the plasma-processed AlO_yF_x layer with this assumed thermal conductivity range of 1 to 35 W m^{-1} K^{-1} yields an Al/AlO_yF_x TBC between 98 and 112 MW m^{-2} K^{-1} for the longest-processed sample. While the aforementioned assumption of asymmetry may not be strictly valid, as plasma processing may produce a slight depth-dependent change in the composition, it would not drastically affect this extracted TBC for Al/AlO_yF_x interfaces. If one were to assume a completely unmodified lower boundary, such that one interface is Al/AlO_yF_x and the second remains an Al/Al_2O_3 interface, the TBC for these Al/AlO_yF_x interfaces at the longest processing time ranges from 58 to 95 MW m^{-2} K^{-1} and thus remains over a factor of two lower than that of an Al/Al_2O_3 interface. Similarly, potential variations in the thickness of the oxyfluoride layer due to plasma processing do not significantly vary the calculated TBC for an Al/AlO_yF_x interface.

To understand this drastic reduction in TBC when comparing an oxide with the fluoride layer, we consider one of the primary factors leading to changes in interfacial heat transfer at the nanoscale: interfacial bonding. The role of bonding has been well studied, with a large number of previous works reporting the effect of bonding on thermal boundary conductance[14,15,35–38] specifically at aluminum/substrate interfaces.[7,39,40] To gain experimental insight into the bond strength between the Al transducer and the passivation layer, we perform picosecond acoustic measurements for the four samples; this method has been described in-depth in numerous works.[15,17,41] In short, this method allows for direct measure of zone-center acoustic phonon propagation in the metal transducer and its dissipation across the substrate interface. Experimentally, an acoustic strain pulse is launched from the Al surface toward the passivation layer. Upon interaction with this interface, the strain pulse partially reflects toward the surface of the film and partially transmits toward the substrate. As the measured reflectivity is sensitive to changes in strain at the surface of the Al film, a "blip" can be observed in the transient reflectance data as this strain pulse reaches the surface [see Fig. 3(a)]. This acoustic wave will then undergo another reflection at the Al/air interface, thus rebounding toward the passivation layer a second time; this process will repeat until the acoustic wave has fully dissipated. Each interaction with the film/substrate interface leads to an exponential decay in the magnitude of this acoustic pulse due to energy transmission across the interface, where the time-dependent intensity of the measured reflectance can be described by the following equation:[17,42]

$$I(t,T) = A * \exp(-\Gamma t)\cos\left(\left(\frac{2\pi}{T}\right)t - \delta\right) - B * \exp\left(-\frac{t}{\tau}\right), \quad (2)$$

where A, B, and δ are scaling factors, Γ is the damping factor of the measured acoustic intensity due to interfacial energy transfer, T is the period in which this acoustic wave reaches the sample surface, and the exponential function accounts for thermal decay through the metal film. The acoustic energy transmission associated with this process can be quantified through this damping factor, Γ, and the periodicity of the observed acoustic blip, T, each obtained from fitting Eq. (2) to the experimental pump-probe data, via

$$\textit{Acoustic transmission} = 1 - \exp(-\Gamma * T). \quad (3)$$

For example, at a well-bonded interface, typically associated with high TBCs, more acoustic energy can be transmitted across the interface, leading to an increase in this acoustic transmission factor.[36] Conversely, in cases where the transducer is poorly bonded to the substrate, one would expect a reduced damping factor and thus acoustic

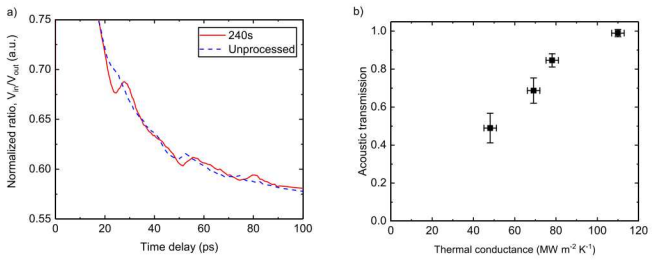

FIG. 3. (a) Measured ratio of the in-phase to out-of-phase signal at early pump-probe time delays for an 80 nm Al/native oxide (Al_2O_3)/80 nm Al film (dashed blue line) and an 80 nm Al/AlO_xF_y/80 nm Al film (straight red line) on a SiO_2 substrate; an acoustic echo can be observed every ~22 picoseconds on the surface of the top Al film. The intensity of this acoustic pulse over time is related to its transmission at the Al/oxide interface, which is proportional to bonding between the two layers. (b) Acoustic transmission as a function of measured thermal conductance across the Al/AlO_yF_x and Al/native oxide interface; a general monotonic increase is observed, implying interfacial bond strength is a dominant factor for the change in TBC observed in the various layers.

transmission across the interface. Indeed, upon comparing the measured acoustic transmission of our Al/AlO_xF_y films with the measured thermal conductance across the passivation layer, we find there is a nearly linear, monotonic trend between the two parameters, as shown in Fig. 3(b). This agreement implies that the passivation layer is weakly bonded to the metal Al film. Through simple inspection of the Ellingham diagram for oxides and fluorides, one can see that the Gibbs free energy associated with aluminum oxide formation is nearly 25% lower (greater magnitude) than that of aluminum fluoride.[43] From this perspective alone, it is not surprising that Al-F bonds would be weaker than Al-O bonds and thus lead to a reduction in metallic film adhesion to the oxyfluoride layer compared to that of the oxide layer alone, ultimately reducing the thermal conductance across the processed layer. We further note that the observed periodicity of the acoustic signal remains unchanged for various processing conditions, indicating there is no measurable change in the thickness of the plasma-processed oxyfluoride layer. Finally, given the low ion energies associated with the plasma, roughness or defect formation is not likely to play a meaningful role in the reduction in thermal conductance or acoustic transmission with increasing plasma processing times. The ability of the LAPPS system to chemically modify materials without plasma induced damage is well documented.[44–46]

In summary, we have experimentally measured the interfacial thermal conductance between an Al film and an AlO_yF_x layer grown via plasma-processing. These values were compared with the TBC of aluminum and its native oxide, which was shown to be in excellent agreement with previous experiments and theories the TBC of Al/AlO_yF_x interfaces is found to be 2 to 3 times lower than that of the Al/native oxide interface. Through picosecond acoustic measurements, it was determined that changes in interfacial bonding are the predominant mechanism for changes in TBC between the layers. These findings have important implications for the use of AlF_xO_y layers as optical films and barrier coatings in battery architectures, as it becomes more necessary to account for thermal accumulation due to the lower conductance of these layers.

J.A.T. and P.E.H. acknowledge support from the Office of Naval Research (Grant No. N00014-15-1-2769). This work was partially supported by the NRL base program through the Office of Naval Research.

REFERENCES

[1]M. Ziegler, J. W. Tomm, D. Reeber, T. Elsaesser, U. Zeimer, H. E. Larsen, P. M. Petersen, and P. E. Andersen, "Catastrophic optical mirror damage in diode lasers monitored during single-pulse operation single-pulse operation," Appl. Phys. Lett. **94**, 191101 (2010).
[2]C. S. Lee, N. Koumvakalis, and M. Bass, "A theoretical model for multiple-pulse laser-induced damage to metal mirrors," Appl. Phys. Lett. **54**, 5727 (2014).
[3]P. B. Corkum, F. Brunel, N. K. Sherman, and T. Srinivasan-Rao, "Thermal response of metals to ultrashort-pulse laser excitation," Phys. Rev. Lett. **61**, 2886–2889 (1988).
[4]J.-P. Tourrenc, S. Bouchoule, A. Khadour, J. Decobert, A. Miard, J. C. Harmand, and J. L. Oudar, "Thermal optimization of 1.55 um OP-VECSEL with hybrid metal-metamorphic mirror for single-mode high power operation," Opt. Quantum Electron. **40**, 155–165 (2008).
[5]J. A. Tomko, A. Giri, B. F. Donovan, D. M. Bubb, S. M. O'Malley, and P. E. Hopkins, "Energy confinement and thermal boundary conductance effects on short-pulsed thermal ablation thresholds in thin films," Phys. Rev. B **96**, 14108 (2017).
[6]Y. Shen, J. Gaskins, X. Xie, B. M. Foley, R. Cheaito, P. E. Hopkins, and J. C. Campbell, "Thermal analysis of high-power flip-chip-bonded photodiodes," J. Lightwave Technol. **35**, 4242–4246 (2017).
[7]E. T. Swartz and R. O. Pohl, "Thermal boundary resistance," Rev. Mod. Phys. **61**, 605–668 (1989).
[8]C. Monachon, L. Weber, and C. Dames, "Thermal boundary conductance: A materials science perspective," Annu. Rev. Mater. Res. **46**, 433–463 (2016).
[9]S. Wilbrandt, O. Stenzel, H. Nakamura, A. Duparré, and N. Kaiser, "Protected and enhanced aluminum mirrors for the VUV," Appl. Opt. **53**, 125–130 (2014).
[10]M. Miles, "Evaporated aluminum fluoride as a barrier layer to retard oxidation of aluminum mirrors," ■ (2017).
[11]N. Gutierrez-Luna, B. Perea-Abarca, L. Espinosa-Yanez, C. Honrado-Benitez, T. de Lis, L. V. Rodriguez-de Marcos, J. A. Aznarez, and J. I. Larruquert, "Temperature dependence of AlF3 protection on far-UV Al mirrors," Coatings **9**, 428 (2019).
[12]M. Mantymaki, M. Ritala, and M. Leskela, "Metal fluorides as lithium-ion battery Materials: An atomic layer deposition perspective," Coatings **8**, 277 (2018).
[13]D. G. Cahill, "Analysis of heat flow in layered structures for time-domain thermoreflectance," Rev. Sci. Instrum. **75**, 5119–5122 (2004).
[14]A. Giri and P. E. Hopkins, "A review of experimental and computational advances in thermal boundary conductance and nanoscale thermal transport across solid interfaces," Adv. Funct. Mater. ■, 1903857 (2019).
[15]M. D. Losego, M. E. Grady, N. R. Sottos, D. G. Cahill, and P. V. Braun, "Effects of chemical bonding on heat transport across interfaces," Nat. Mater. **11**, 502–506 (2012).
[16]C. S. Gorham, K. Hattar, R. Cheaito, J. C. Duda, J. T. Gaskins, T. E. Beechem, J. F. Ihlefeld, L. B. Biedermann, E. S. Piekos, D. L. Medlin, and P. E. Hopkins, "Ion irradiation of the native oxide/silicon surface increases the thermal boundary conductance across aluminum/silicon interfaces," Phys. Rev. B **90**, 24301 (2014).
[17]J. A. Tomko, D. H. Olson, A. Giri, J. T. Gaskins, B. F. Donovan, S. M. O'Malley, and P. E. Hopkins, "Nanoscale wetting and energy transmission at solid/liquid interfaces," Langmuir **35**, 2106–2114 (2019).
[18]W. M. Manheimer, R. F. Fernsler, M. Lampe, and R. A. Meger, "Theoretical overview of the large-area plasma processing system (LAPPS)," Plasma Sources Sci. Technol. **9**, 370–386 (2000).
[19]R. A. Meger, R. F. Fernsler, M. Lampe, and W. Manheimer, Large Area Plasma Process. Syst. **5**, 984807 (1999).
[20]G. M. Petrov, D. R. Boris, E. H. Lock, T. B. Petrova, R. F. Fernsler, and S. G. Walton, "The influence of magnetic field on electron beam generated plasmas," J. Phys. D Appl. Phys. **48**, 275202–275208 (2015).
[21]S. G. Walton, D. R. Boris, S. C. Hernandez, E. H. Lock, T. B. Petrova, G. M. Petrov, and R. F. Fernsler, "Electron beam generated plasmas for ultra low Te processing," ECS J. Solid State Sci. Technol. **4**, N5033––N5040 (2015).
[22]D. R. Boris and S. G. Walton, "Precise control of ion and radical production using electron beam generated plasmas," J. Vac. Sci. Technol., A. **36**, 60601 (2018).
[23]D. R. Boris, R. F. Fernsler, and S. G. Walton, "Measuring the electron density, temperature, and electronegativity in electron beam-generated plasmas produced in argon/SF6 mixtures," Plasma Sources Sci. Technol. **24**, 25032 (2015).
[24]D. R. Boris, T. B. Petrova, G. M. Petrov, and S. G. Walton, "Atomic fluorine densities in electron beam generated plasmas: A high ion to radical ratio source for etching with atomic level precision," J. Vac. Sci. Technol., A **35**, 01A104 (2017).
[25]S. M. George and Y. Yee, "Prospects for thermal atomic layer etching using sequential, self-limiting fluorination and ligand-exchange reactions," ACS Nano **10**, 4889–4894 (2016).
[26]S. K. Natarajan and S. D. Elliott, "Modeling the chemical mechanism of the thermal atomic layer etch of aluminum oxide: A density functional theory study of reactions during HF exposure," Chem. Mater. **30**, 5912–5922 (2018).
[27]S. G. Walton, S. C. Hernandez, D. R. Boris, T. B. Petrova, and G. M. Petrov, "Electron beam generated plasmas for the processing of graphene," J. Phys. D: Appl. Phys. **50**, 354001––354017 (2017).

[28]S. G. Walton, E. H. Lock, A. Ni, M. Baraket, R. F. Fernsler, D. D. Pappas, K. E. Strawhecker, and A. A. Bujanda, "Study of plasma-polyethylene interactions using electron beam generated plasmas produced in Ar/SF6 mixtures," J. Appl. Polym. Sci. **117**, 3515 (2010).
[29]D. G. Cahill, S.-M. Lee, and T. I. Selinder, "Thermal conductivity of k-Al_2O_3 and aAl_2O_3 wear-resistant coatings," J. Appl. Phys. **83**, 5783 (1998).
[30]Y. Lee, J. W. Dumont, A. S. Cavanagh, and S. M. George, "Atomic layer deposition of AlF 3 using trimethylaluminum and hydrogen fluoride," J. Phys. Chem. C **119**, 14185–14194 (2015).
[31]C.-C. Lee, M.-C. Liu, M. Kaneko, K. Nakahira, and Y. Takano, "Characterization of AlF3 thin films at 193 nm by thermal evaporation," Appl. Opt. **44**, 7333–7338 (2005).
[32]W. Heitmann, "Vacuum evaporated films of aluminum fluoride," Thin Solid Films **800**, 61–67 (1969).
[33]K. Iwahori, M. Furuta, Y. Taki, T. Yamamura, and A. Tanaka, "Optical properties of fluoride thin films deposited by RF magnetron sputtering," Appl. Opt. **45**, 4598–4602 (2006).
[34]D. G. Cahill, S. K. Watson, and R. O. Pohl, "Lower limit to the thermal conductivity of disordered crystals," Phys. Rev. B **46**, 6131–6140 (1992).
[35]M. Shen, W. J. Evans, D. Cahill, and P. Keblinski, "Bonding and pressure-tunable interfacial thermal conductance," Phys. Rev. B **84**, 195432 (2011).
[36]G. Tas, J. J. Loomis, H. J. Maris, A. A. Bailes, and L. E. Seiberling, "Picosecond ultrasonics study of the modification of interfacial bonding by ion implantation," Appl. Phys. Lett. **72**, 2235 (1998).
[37]H. Harikrishna, W. A. Ducker, and S. T. Huxtable, "The influence of interface bonding on thermal transport through solid-liquid interfaces," Appl. Phys. Lett. **102**, 251606 (2013).
[38]P. E. Hopkins, "Thermal transport across solid interfaces with nanoscale imperfections: Effects of roughness, disorder, dislocations, and bonding on thermal boundary conductance," ISRN Mech. Eng. **2013**, 1–19 (2013).
[39]G. T. Hohensee, R. B. Wilson, and D. G. Cahill, "Thermal conductance of metaldiamond interfaces at high pressure," Nat. Commun. **6**, 1–9 (2015).
[40]P. E. Hopkins, M. Baraket, E. V. Barnat, T. E. Beechem, S. P. Kearney, J. C. Duda, J. T. Robinson, and S. G. Walton, "Manipulating thermal conductance at metal-graphene contacts via chemical functionalization," Nano Lett. **12**, 590–595 (2012).
[41]C. Thomsen, H. T. Grahn, H. J. Maris, and J. Tauc, "Surface generation and detection of phonons by picosecond light pulses," Phys. Rev. B **34**, 4129 (1986).
[42]J. C. Duda, C.-Y. P. Yang, B. M. Foley, R. Cheaito, D. L. Medlin, R. E. Jones, and P. E. Hopkins, "Influence of interfacial properties on thermal transport at gold: Silicon contacts," Appl. Phys. Lett. **102**, 81902 (2013).
[43]T. B. Reed, *Free Energy of Formation of Binary Compounds* (MIT Press, 1971).
[44]A. V. Jagtiani, H. Miyazoe, J. Chang, D. B. Farmer, M. Engel, D. Neumayer, S.-J. Han, S. U. Engelmann, D. R. Boris, S. C. Hernandez, E. H. Lock, S. G. Walton, and E. A. Joseph, "Initial evaluation and comparison of plasma damage to atomic layer carbon materials using conventional and low Te plasma sources," J. Vac. Sci. Technol., A **34**, 01B103 (2016).
[45]E. H. Lock, D. Y. Petrovykh, P. Mack, T. Carney, R. G. White, S. G. Walton, and R. F. Fernsler, "Surface composition, chemistry, and structure of polystyrene modified by electron-beam-generated plasma," Langmuir **26**, 8857–8868 (2010).
[46]B. J. Orf, S. G. Walton, D. Leonhardt, and G. S. Oehrlein, "Study of photoresist etching and roughness formation in electron-beam generated plasmas," J. Vac. Sci. Technol., B **25**, 779 (2007).